



Presumed Little Ice Age glacial extent in the eastern Tian Shan, China

Yanan Li, Yingkui Li, Yixin Chen & Xiaoyu Lu

To cite this article: Yanan Li, Yingkui Li, Yixin Chen & Xiaoyu Lu (2016) Presumed Little Ice Age glacial extent in the eastern Tian Shan, China, Journal of Maps, 12:sup1, 71-78, DOI: [10.1080/17445647.2016.1158595](https://doi.org/10.1080/17445647.2016.1158595)

To link to this article: <https://doi.org/10.1080/17445647.2016.1158595>



© 2016 Yingkui Li



View supplementary material [↗](#)



Published online: 16 Mar 2016.



Submit your article to this journal [↗](#)



Article views: 469



View Crossmark data [↗](#)



Citing articles: 3 View citing articles [↗](#)



SCIENCE

Presumed Little Ice Age glacial extent in the eastern Tian Shan, China

Yanan Li^a , Yingkui Li^a, Yixin Chen^b and Xiaoyu Lu^a

^aDepartment of Geography, University of Tennessee, Knoxville, TN, USA; ^bCollege of Urban and Environmental Sciences, Peking University, Beijing, People's Republic of China

ABSTRACT

Mountain glaciers across the Tian Shan provide critical freshwater resources for the arid and semi-arid areas in Central Asia. Glacial extent during the Little Ice Age (LIA) has been investigated in individual valleys, but its spatial characteristic across a large region still remains unclear. We delineated the presumed maximum LIA glacial extents in three study regions of the eastern Tian Shan (the Boro-Eren, the Bogeda, and the Barkol-Karlik ranges) using Google Earth and the 30 m Shuttle Radar Topography Mission digital elevation model. The corresponding contemporary glaciers were extracted from the Second Glacier Inventory Dataset of China. The total area of 865 contemporary glaciers was estimated to cover 791.6 km² during a LIA Maximum and decreased to 484.6 km² around 2006–2010, with a relative area loss of 38.8%. The spatial pattern of glacier area loss exhibits a west–east decreasing trend between these three regions. This map provides a data set to investigate the pattern of LIA glacial extents and assess climate impact on water resources in the eastern Tian Shan at a centennial time scale.

ARTICLE HISTORY

Received 23 October 2015
Revised 12 February 2016
Accepted 21 February 2016

KEYWORDS

Little Ice Age; marginal moraine; the Second Glacier Inventory of China; eastern Tian Shan

1. Introduction

Meltwater from mountain glaciers provides critical freshwater resources for populated lowlands in Kyrgyzstan, Kazakhstan, Uzbekistan, and northwestern China in Central Asia (Aizen, 2011; Farinotti et al., 2015). The Tian Shan, a major mountain range and known as the 'Water Tower of Central Asia' (Sorg, Bolch, Stoffel, Solomina, & Beniston, 2012), consists of a large glacier repository in this arid and semi-arid region. It stretches approximately 2500 km west–east from the western boundary of Kyrgyzstan to Xinjiang Uyghur Autonomous Region in China, and almost reaching Mongolia (Figure 1). Reconstructing the pattern of glacier changes is critical to understand global and regional climate change and assess the impact of climate change on regional water resources, ranging from residential, agricultural, and industrial water uses to building national defense infrastructure (Gao, Han, Ye, & Jiao, 2013; Lioubimtseva & Henebry, 2009; Solomina & Alverson, 2004). A number of studies have investigated the timing and extent of past glaciations in the Tian Shan for individual locations (e.g. Chen et al., 2015; Koppes, Gillespie, Burke, Thompson, & Stone, 2008; Li et al., 2011, 2014; Narama et al., 2007; Zhao, Zhou, He, Ye, & Liu, 2006; Zech, 2012). With the advance of remote sensing technology, geomorphological mapping was also provided in conjunction with these site-specific glacial investigations. Stroeven, Hättestrand, Heyman, Kleman, and Morén (2013) presented a regional map of glacial geomorphology across the

Tian Shan. This map includes various glacial landforms and a series of marginal moraines to indicate the extents of multiple glacial stages. However, the focus of this published map was mainly on glacial events prior to the Holocene; the glacial extent during the late Holocene, in particular, the Little Ice Age (LIA), and the glacial retreat pattern since then, were not illustrated.

The concept of the LIA was first introduced by Matthes (1939) to describe glacial advances to an extensive position after the warm epoch of the mid-Holocene and before the twentieth century. Abundant evidence, including tree rings, sediments, and ice cores, has revealed a cold and wet climate during the LIA in Central Asia (e.g. Chen, Huang, Zhang, Holmes, & Chen, 2006; Esper et al., 2003; Liu & Han, 1992). The map presented here (Main Map) focuses on the maximum glacial extent during the LIA in the eastern Tian Shan. Previous studies suggest that glaciers reached their LIA maximum extent at different cold periods during the last millennium (Chenet, Rousset, Jomelli, & Grancher, 2010; Liu, Sun, Shen, & Li, 2003; Xu & Yi, 2014), and have been retreating since the end of the LIA around AD 1850 (Grove, 2004; Matthews & Briffa, 2005; Sorg et al., 2012). Various techniques have been applied to constrain the age of presumed LIA moraines in the Tian Shan (Chen, 1989; Chen et al., 2015; Koppes et al., 2008; Li et al., 2014; Solomina, Barry, & Bodnya, 2004; Yi et al., 2004). For example, at the Urumqi River headwaters (Figure 2),

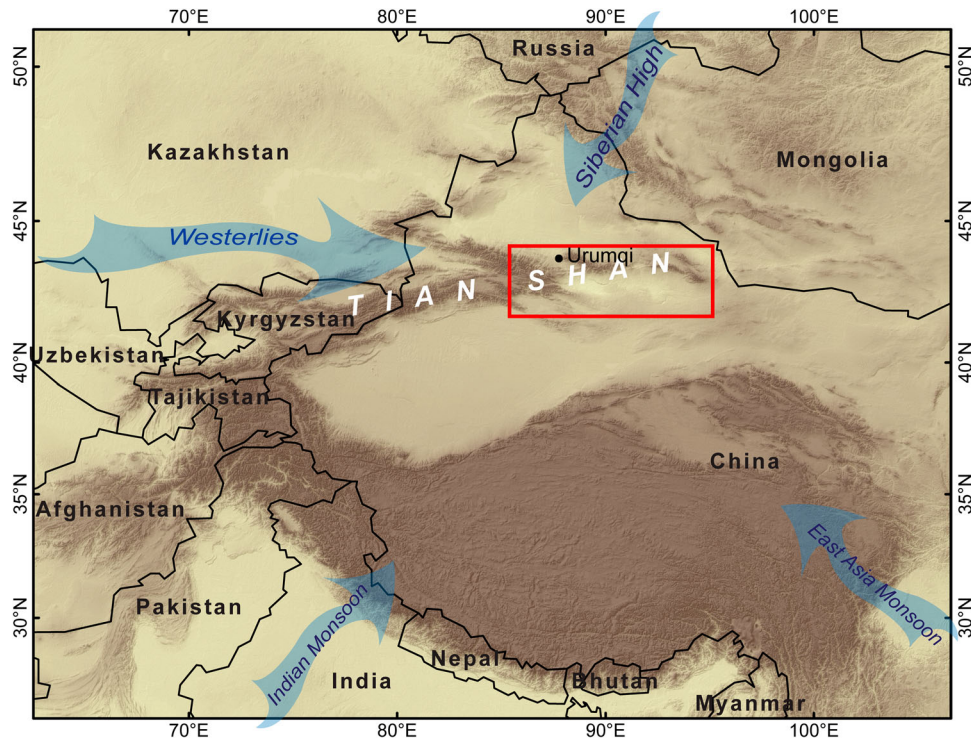


Figure 1. Overview map showing the location of the study area (red box) and surrounding climate systems (blue arrows).

fresh-looking moraines in front of Glacier No. 1 have been constrained to LIA ages using lichenometry (Chen, 1989), AMS ^{14}C dating (Yi et al., 2004), and cosmogenic ^{10}Be exposure dating (Li et al., 2014). In the easternmost Tian Shan, Chen et al. (2015) constrained the LIA moraines based on ^{10}Be exposure dating. In the western Tian Shan, Koppes et al. (2008) reported two LIA ^{10}Be exposure ages from moraines in the Kyrgyz Front Range. Xu and Yi (2014) summarized chronologies of the LIA moraines on the Tibetan Plateau (TP) and surrounding mountains, including the Tian Shan, and noted that most glaciers in the northwestern TP advanced to their LIA maximum earlier than in the southern TP in the fourteenth century. Although LIA

glacial events have been constrained at these individual sites, the spatial pattern of the LIA glacial extents is still lacking, especially in the eastern Tian Shan that was not fully included in the previous mapping (Stroeven et al., 2013). In combination with previous knowledge of the dated LIA extents, this map would be useful in studying glacier dynamics and examining spatial characteristics of past ice extents at a centennial time scale.

2. Study area

Our study area is the eastern Tian Shan, ranging from approximately $85^{\circ}40'\text{E}$ to $94^{\circ}50'\text{E}$ and from $42^{\circ}40'\text{N}$ to $44^{\circ}00'\text{N}$, and stretching about 800 km in length with

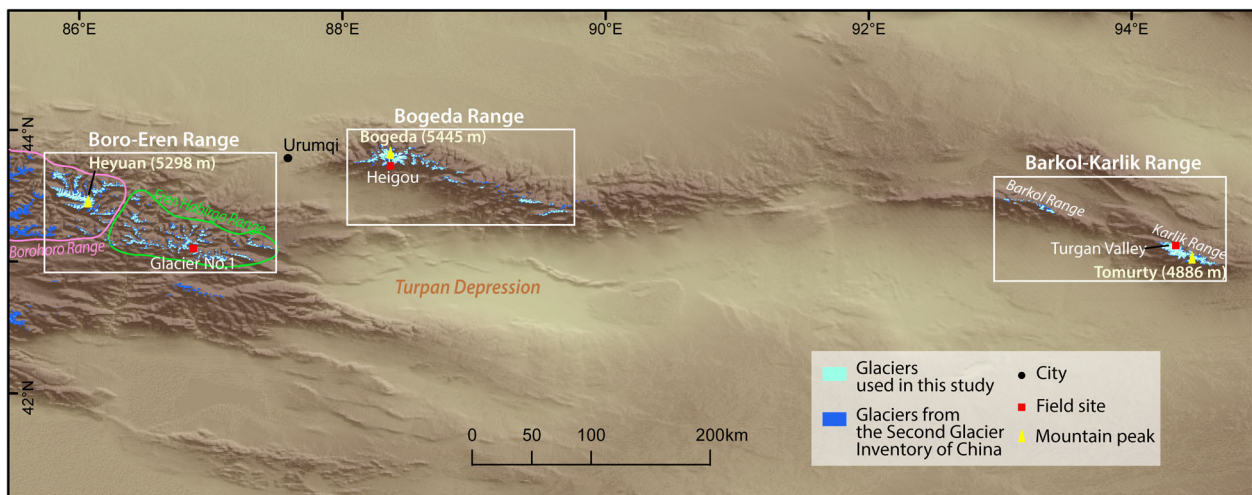


Figure 2. Three study regions in the eastern Tian Shan. Field sites of the Urumqi River headwaters, the Heigou Valley, and the Turgan Valley are illustrated as red dots.

an area of ca. 154,000 km². Mountain glaciers are developed at high elevations of >3000 m above sea level (a.s.l.). The mid-latitude westerlies and the Siberian High are the main climate systems in this area, providing precipitation and temperature conditions to maintain the mass balances of the glaciers; while the Asian monsoon systems hardly penetrate here due to the orographic barriers of the Himalayas and the TP (Aizen, Aizen, Melack, Nakamura, & Ohta, 2001; Benn & Owen, 1998; Sorg et al., 2012; Figure 1).

We define three study regions from west to east (Figure 2) based on their geographic locations. The first region is the Boro-Eren Range, including the

eastern Borohoro and the Eren Habirga ranges. The second region is the Bogeda Range, located north of the Turpan Depression and 50 km east of Urumqi, the capital city of Xinjiang Uyghur Autonomous Region, China. The third region is the Barkol-Karlik Range, located at the easternmost end of the Tian Shan, including the Barkol and Karlik ranges. The highest peaks are Mt. Heyuan (5298 m a.s.l.), Mt. Bogeda (5445 m a.s.l.), and Mt. Tomurty (4886 m a.s.l.), for the three regions. Abundant glacial landforms have been identified in these regions, including U-shaped valleys, cirques, moraines, and striations (Cui, Xiong, Liu, Zhu, & Yi, 1998; Figure 3).

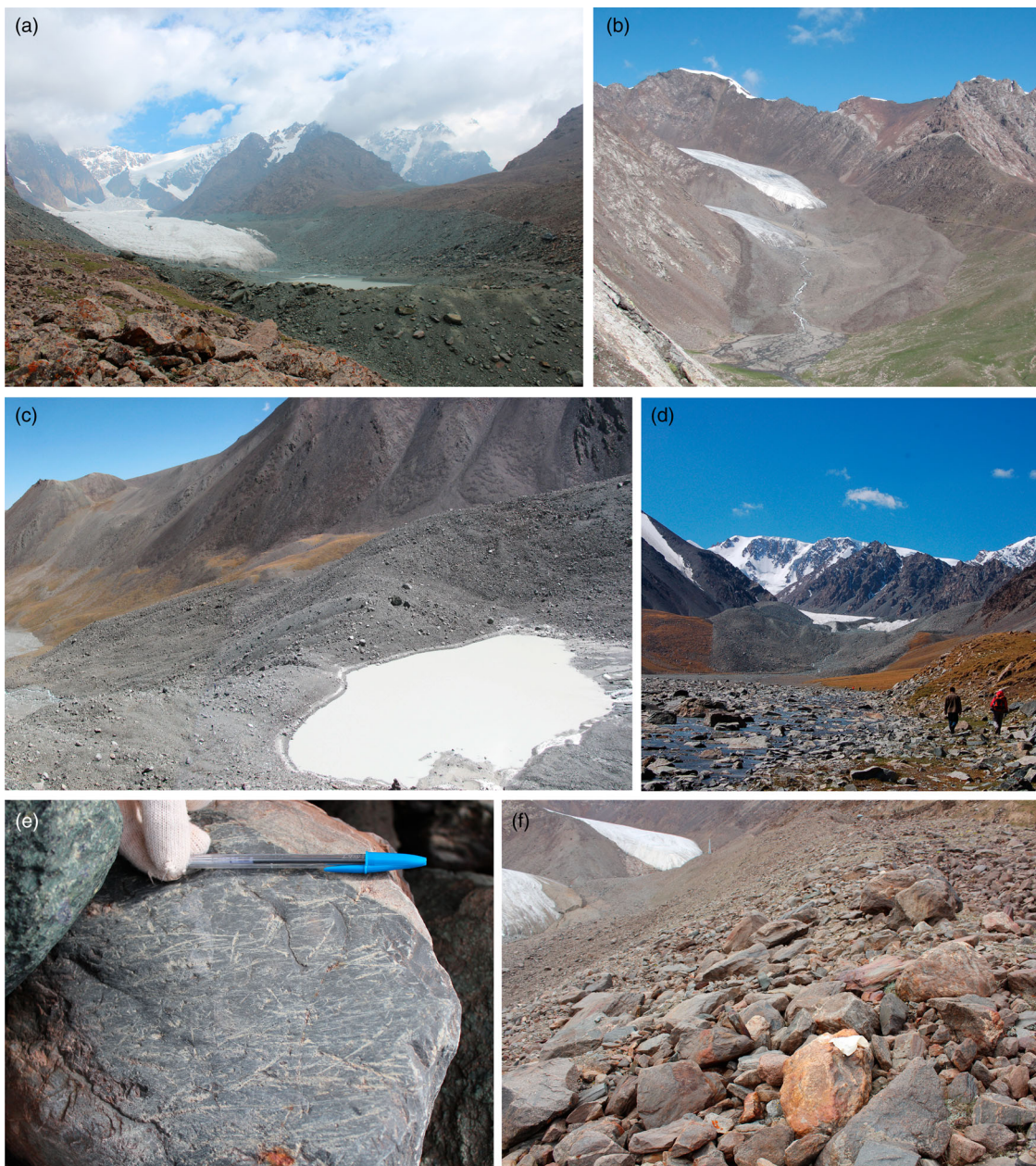


Figure 3. Field photos of glacial landforms and features: (a) fresh-looking LIA moraines in the Heigou Valley; (b) LIA moraine in front of Glacier No. 1 at the Urumqi River headwaters; (c) a pond dammed by LIA moraines at the Turgan Valley; (d) fresh-looking LIA moraines overlay vegetated older landforms at the Turgan Valley; (e) striations; (f) a close-up view of boulders on top of the fresh moraine at the Glacier No. 1 site.

3. Methods

3.1. Data sources

Google Earth high-resolution imagery was utilized as the major source to map the LIA glacial extents. In recent years, Google Earth has become a popular platform for visualizing various types of remote sensing data, such as Landsat, SPOT, IKONOS, GeoEye, and DigitalGlobe, in a 3D and interactive manner (Sun et al., 2012; Yu & Gong, 2012). The enhanced 3D and interactive visualization make Google Earth a unique platform for landform mapping, even though the acquisition date and spatial resolution of the imagery may vary from place to place (Butler, 2006). Google Earth also provides historical imagery, allowing an easy check on the availability of alternative imagery with better resolution in the area of interest. In this study, LIA glacial landforms were identified and delineated using the best available imagery in Google Earth (most images are from DigitalGlobe®).

The other data source used for mapping is the Shuttle Radar Topography Mission (SRTM) 1 arc-second digital elevation model (DEM), downloaded from the USGS Earth Explorer (<http://earthexplorer.usgs.gov>). This DEM is about 30 m resolution and was clipped to the mapping area to help identify and calculate landform characteristics.

The contemporary glaciers in the eastern Tian Shan were extracted from the Second Glacier Inventory of China (Guo et al., 2014). As part of the world glacier inventory of the Global Land and Ice Measurements from Space (GLIMS) project (Paul et al., 2009), the Second Glacier Inventory of China provides data sources and attributes for each individual glacier in China. The glacier boundary was delineated based on Landsat TM/ETM+ scenes acquired between 2006 and 2010 using band ratios and was manually checked against topographic maps, ASTER images, and Google Earth. The uncertainty of the delineated glacier boundary is about ± 30 m, comparable to one pixel size of the Landsat TM/ETM+ imagery (Guo et al., 2014).

3.2. Mapping procedure

LIA moraines in the Tian Shan are commonly identified as fresh, bouldery, and sharp-crested moraines located within a few hundred to thousand meters away from the present glacier terminus (Shi & Ren, 1990; Solomina et al., 2004; Figure 3). In western China, some LIA moraine sets include two or three lateral/terminal moraine ridges, indicating multiple glacial events during the LIA (Liu et al., 2003; Shi & Ren, 1990; Xu & Yi, 2014). We define the outermost fresh moraine to represent the maximum extent of LIA glaciers. We interpret potential LIA features according to their geomorphic location/relationship,

morphology, vegetation cover, and weathering characteristics. Marginal moraines, including terminal and lateral moraines, of LIA glaciers are typically deposited within glacial valleys, while some developed in the tributary valleys and can extend to the main valley floor in the eastern Tian Shan. In addition, most LIA moraine ridges appear to override vegetated, gentle, and old-looking moraines to form a distinct boundary (Figure 3(a)–(d)). Moraine-dammed lakes are occasionally present between fresh moraine ridges and the contemporary glaciers (Figure 3(a) and 3(c)). Meltwater from glaciers also cuts through some parts of the marginal moraine, causing a low degree of degradation (Figure 3(b)).

The delineated LIA moraines were saved as KML files from Google Earth and converted into shapefiles. Polygons of LIA glacial extents were derived from overlapping the delineated LIA marginal moraine with its corresponding contemporary glacier(s) (Figure 4). Only contemporary glaciers with LIA glacial extents were exported as a polygon shapefile and were presented in the final map product. Note that one particular LIA extent may correspond to several contemporary glaciers due to ice retreat.

To produce the final map, the SRTM 1 arc-second DEM and contemporary and LIA glacial extents were integrated in ArcGIS 10.1 and projected to the Universal Transverse Mercator coordinate system, zone 45 N, in datum WGS1984 (see Supplementary Materials). Hillshaded relief was produced with 60% transparency and stacked under the DEM layer that was set with 30% transparency.

3.3. Accuracy assessment

We visited several glacial valleys in the three regions to validate the mapping results and assessed the accuracy of the delineated LIA extents during two field trips in 2009 and 2012. In the Urumqi River headwater area in the Boro-Eren Range, we visited Glacier No. 1 and other surrounding glaciers and recorded 15 coordinates using a global positioning system (GPS) receiver on top of LIA moraines (Figure 4(a)). In the Bogeda Range, we recorded a GPS receiver track by walking on top of the LIA moraine in the Heigou Valley on the southern slope of Mt. Bogeda (Figure 4(b)). In the Karlik Range, fresh moraines in front of two valley glaciers in the Turgan Valley were examined and dated to the LIA period (Chen et al., 2015; Figure 4(c)).

We applied a revised automated proximity and conformity analysis (Li, Napieralski, & Harbor, 2008) to quantify the offset between the GPS receiver measurements and mapped LIA extents. The offsets between 15 GPS-located points and their corresponding delineated boundaries at Glacier No. 1 range from 1.8 to 18.8 m, with an average of 10.5 m; the average offset between the GPS track and the delineated LIA boundary in

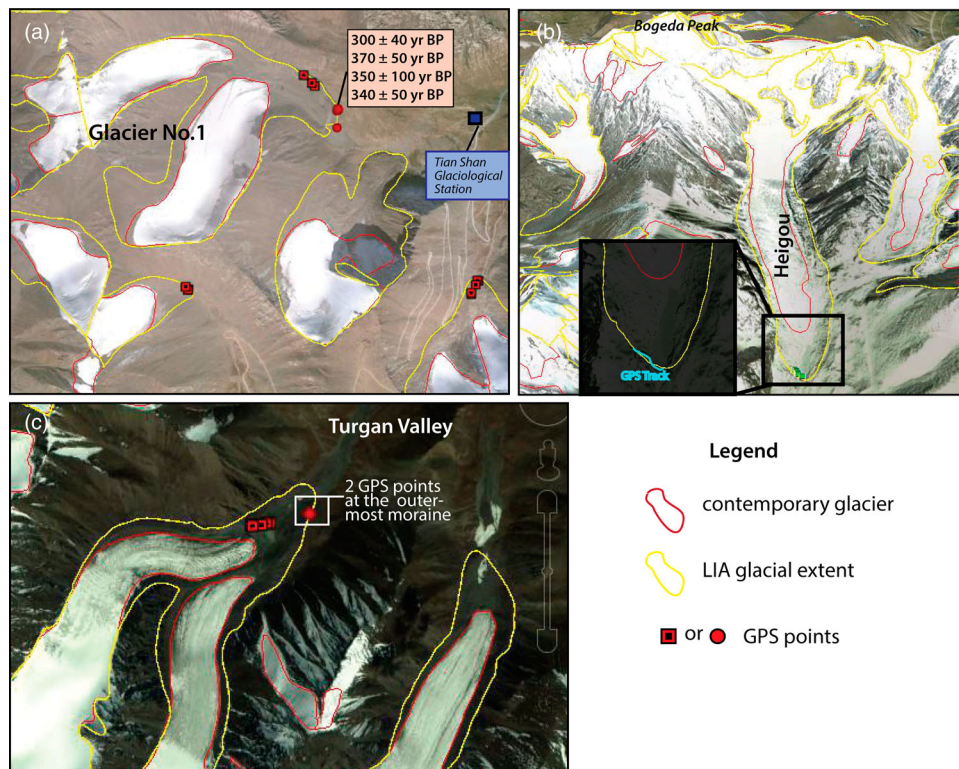


Figure 4. Google Earth view of three areas with field validation: (a) the Urumqi river headwaters area in the Boro-Eren study region, with 15 GPS receiver points. Four ages in the box are derived using cosmogenic ¹⁰Be ages calculated with the Lal/Stone time-dependent production rate in Li et al. (2014) with 60 years correction to make them compatible to the unit of year BP (year before 1950); (b) the Heigou Valley in the Bogeda study region, with a GPS receiver track route (blue line in the inset graph) lined up with the LIA glacial boundary (in yellow); (c) the Turgan Valley in the Karlik study region, with two GPS receiver points located at the outermost moraine. The background images are screenshots of Google Earth imagery.

Heigou Valley is about 9.4 m; and the two GPS coordinates in the Turgan Valley are within 5.0 and 13.2 m of the delineated LIA outline. All these offsets are within one pixel size (~30 m) of the Landsat TM/ETM+ imagery, a commonly used image source for glacier delineation (e.g. Bhambri, Bolch, Chaujar, & Kulshreshtha, 2011; Bolch, 2007; Paul, Huggel, & Kääb, 2004). Therefore, the accuracy of our delineated LIA boundaries (~10 m) is acceptable for the glacial landform mapping purpose.

4. Landform descriptions

4.1. Contemporary glaciers

The map presented 865 contemporary glaciers in association with the presumed LIA glacial extents in the eastern Tian Shan (Main Map). These glaciers have a total area of 484.6 km² (Table 1). Among the three regions, the Boro-Eren Range contains the most glaciers which account for about half of the total glacier area; the glacier areas in the Bogeda and Barkol-Karlik ranges are similar, although the Barkol-Karlik Range contains only 122 glaciers, 80 less than in the Bogeda Range (Table 1). Among the 865 glaciers, the glacier area ranges from 0.01 km² (in the Bogeda Range) to 9.67 km² (also in the Bogeda Range), and 760 of the

Table 1. Descriptive statistics of glaciers and percentages of glacier area loss between the LIA and present (2006–2010) in the study regions.

| | Boro-Eren | Bogeda | Barkol-Karlik | Overall |
|-------------------------------|-----------|--------|---------------|---------|
| Contemporary glaciers | | | | |
| Number | 541 | 202 | 122 | 865 |
| Total area (km ²) | 244.2 | 128.9 | 111.5 | 484.6 |
| LIA extents | | | | |
| Number | 397 | 169 | 81 | 647 |
| Total area (km ²) | 432.1 | 201.1 | 158.4 | 791.6 |
| Estimated area change (%) | 43.5% | 35.9% | 29.6% | 38.8% |

865 glaciers are <1 km². Specifically, such small glaciers (<1 km²) account for 91.5% of the glacier area in the Boro-Eren Range, 85.6% in the Bogeda Range, and 75.4% in the Barkol-Karlik Range.

Most contemporary glaciers are valley glaciers (at high elevations in the U-shaped valleys), hanging glaciers, and cirque glaciers. The latter two are both frequently found dispersing individually close to mountain ridges. These glaciers are mainly northerly facing as they receive less incoming solar radiation and preserve snow/ice better than the southerly facing glaciers (Li & Li, 2014). In addition, glaciers in the eastern Tian Shan are mostly clear-ice glaciers. Among these 865 glaciers, only 9 glaciers are recorded with debris cover in the Second Glacier Inventory of China (see Supplementary Materials).

4.2. LIA glacial extents

In the eastern Tian Shan, we mapped 640 presumed maximum LIA glacial extents in front of corresponding contemporary glaciers. The total area of the delineated LIA glacial extents is approximately 791.6 km² in three regions (Table 1). Overall, the total glacial extent has reduced by 307.0 km² (38.8%) from their LIA maximum to contemporary extents. Specifically, the reduction in glacier area is about 43.5%, 35.9%, and 29.6%, in the Boro-Eren Range, the Bogeda Range, and the Barkol-Karlik Range, respectively, indicating a west to east decreasing trend in glacier loss. These percentages most likely represent the minimum estimates of glacier area loss because they are based on our delineations in front of 865 glaciers, while some glaciers that may have completely disappeared (100% of area loss) and left only ice-free catchments today are not included in the calculation. Also, note that it is difficult to identify LIA moraines in front of some small glaciers that reside on steep slopes. The delineation of some moraines might also be prevented by the poor quality of Google Earth images, such as cloud cover, shadow, and coarse resolutions found in some areas (Figure 5), but as Google Earth regularly updates image scenes with better quality, the identification of landforms in these areas could be re-checked and improved in the future. Thus, at the time of this study, we only focused on mapping the moraines that could be clearly identified in Google Earth with the characteristics mentioned above.

5. Conclusions

We produced a geomorphological map of presumed LIA glacial extents in the eastern Tian Shan, with a focus on three regions: the Boro-Eren Range, the Bogeda Range, and the Barkol-Karlik Range (Main Map). Based on SRTM DEM and Google Earth data, we manually delineated 640 LIA outermost moraines to represent the maximum LIA glacial extents in different valleys. These LIA glacial extents correspond to 865 contemporary glaciers extracted from the Second Glacier Inventory of China. Field validation using a GPS receiver indicates that the offsets between field measurements and our delineations are about 10 m, lower than or comparable to the uncertainty of glacier extraction commonly derived using Landsat TM/ETM + imagery.

This map provides a useful dataset to understand climate change over last several hundred years in this critical region. In particular, the map illustrates the spatial distribution of LIA glacial extents that can be used to estimate the pattern of glacial retreat since the LIA. The total area loss is estimated to be about 307.0 km² from the LIA to 2006–2010, about 38.8% of the area of mapped LIA glaciers. Estimates of relative glacier area change in the three study regions from west to east are 43.5%, 35.9%, and 29.6%, respectively. These estimates are likely minimum because some glaciers that may have completely disappeared today were not included in the calculation. This decreasing trend may be related to the proportion of small glaciers that tend to have a relatively large percentage of glacier

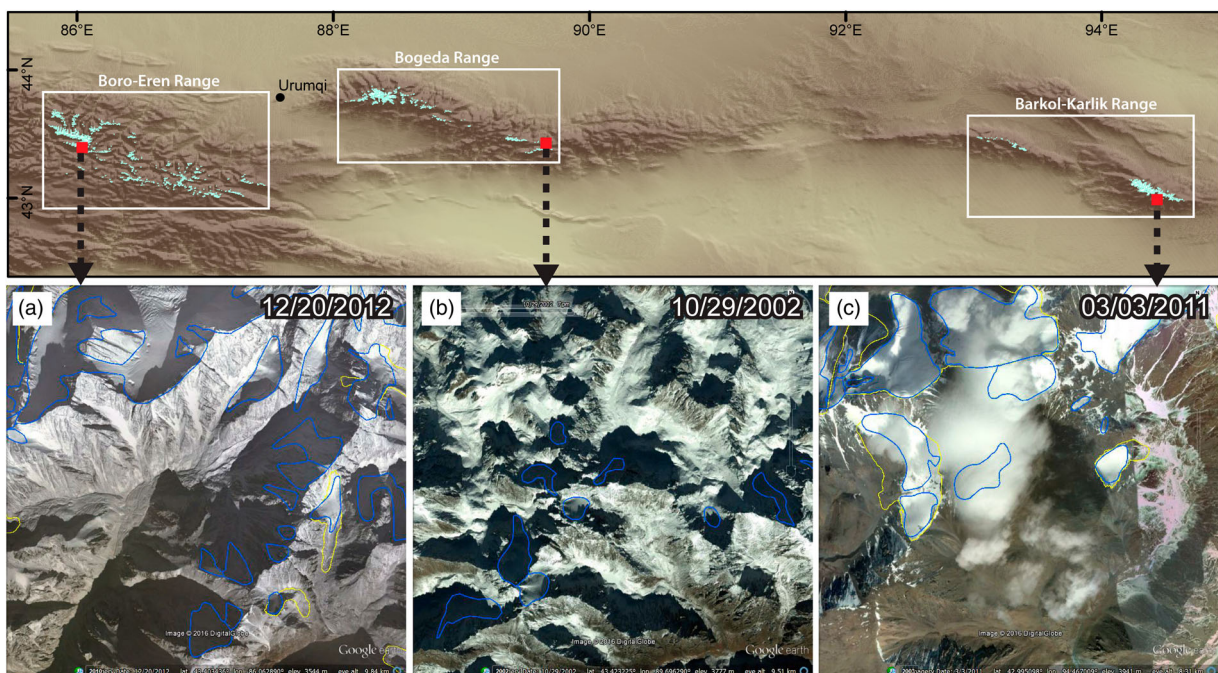


Figure 5. Illustration of difficulties in identifying presumed LIA moraines (yellow lines) due to poor Google Earth imagery at the time of delineation. (a) and (b) show the disturbing effects from shadow and snow cover; (c) shows cloud cover blocking the land surface view.

loss (Bhambri et al., 2011; Khromova, Dyurgerov, & Barry, 2003; Li & Li, 2014; Liu et al., 2003). Other factors, such as climate and/or topographic controls, may also play a role in the observed patterns of glacier retreat between these regions, and more studies are required to quantify the impact of these factors.

Software

Google Earth provided the 3D visualization and an interactive interface to delineate glacial landforms. Esri ArcGIS 10.1 was used to process the DEMs and map layers. Adobe Illustrator CS6 was used to design the map.

Acknowledgements

We thank Gengnian Liu, Mei Zhang, Jingchun Zhang, Xiulin Shen, and Junxi Kang for the field assistance, Yang Xu for helping with the GIS analysis. We also appreciate Carol Harden and Henri Grissino-Mayer for the improvement of the writing. We thank Arjen Stroeven, Elisabeth Mayr, and Heike Apps for their helpful comments and suggestions.

Disclosure statement

No potential conflict of interest was reported by the authors.

Funding

Funding for this work was provided by the National Science Foundation of China [41328001], [40971002]; National Geographic Society Young Explorers [9086-12]; National Science Foundation's Doctoral Dissertation Improvement Research [BCS-1303175].

ORCID

Yanan Li  <http://orcid.org/0000-0002-9456-4514>

References

- Aizen, E. M., Aizen, V. B., Melack, J. M., Nakamura, T., & Ohta, T. (2001). Precipitation and atmospheric circulation patterns at mid-latitudes of Asia. *International Journal of Climatology*, 21(5), 535–556.
- Aizen, V. (2011). 'Tian Shan Glaciers' *Encyclopedia of Earth Sciences Series: Encyclopedia of snow, ice and glaciers* (Singh, V. P., Singh, P., & Haritashya, eds.). Dordrecht, The Netherlands: Springer.
- Benn, D. I., & Owen, L. A. (1998). The role of the Indian summer monsoon and the mid-latitude westerlies in Himalayan glaciation: Review and speculative discussion. *Journal of the Geological Society*, 155, 353–363.
- Bhambri, R., Bolch, T., Chaujar, R. K., & Kulshreshtha, S. C. (2011). Glacier changes in the Garhwal Himalaya, India, from 1968 to 2006 based on remote sensing. *Journal of Glaciology*, 57(203), 543–556.
- Bolch, T. (2007). Climate change and glacier retreat in northern Tien Shan (Kazakhstan /Kyrgyzstan) using remote-sensing data. *Global and Planetary Change*, 56(1–2), 1–12.
- Butler, D. (2006). Virtual globes: The web-wide world. *Nature*, 439, 776–778.
- Chen, F. H., Huang, X. Z., Zhang, J. W., Holmes, J. A., & Chen, J. H. (2006). Humid Little Ice Age in arid central Asia documented by Bosten Lake, Xinjiang, China. *Science in China Series D: Earth Sciences*, 49(12), 1280–1290.
- Chen, J. Y. (1989). The preliminary studies of several problems on lichenometry of glacial variation in the Holocene at the headwaters of the Urumqi River. *Science in China (Series B)*, 1, 95–104.
- Chen, Y. X., Li, Y. K., Wang, Y., Zhang, M., Cui, Z. J., Yi, C. L., & Liu, G. N. (2015). Late Quaternary glacial history of the Karlik Range, easternmost Tian Shan, derived from ¹⁰Be surface exposure and optically stimulated luminescence datings. *Quaternary Science Reviews*, 115, 17–27.
- Chenet, M., Roussel, E., Jomelli, V., & Grancher, D. (2010). Asynchronous Little Ice Age glacial maximum extent in southeast Iceland. *Geomorphology*, 114(3), 253–260.
- Cui, Z. J., Xiong, H. G., Liu, G. N., Zhu, C., & Yi, C. L. (1998). *Landform Processes and Sedimentary Features on the Cryosphere of the Central Tianshan*. Hebei: Hebei Science & Technology Publishing House.
- Esper, J., Shiyatov, S. G., Mazepa, V. S., Wilson, R. J. S., Graybill, D. A., & Funkhouser, G. (2003). Temperature-sensitive Tien Shan tree ring chronologies show multi-centennial growth trends. *Climate Dynamics*, 21, 699–706.
- Farinotti, D., Longuevergne, L., Moholdt, G., Duethmann, D., Molg, T., Bolch, T., ... Guntner, A. (2015). Substantial glacier mass loss in the Tien Shan over the past 50 years. *Nature Geoscience*, 8, 716–722.
- Gao, M. J., Han, T. D., Ye, B. S., & Jiao, K. Q. (2013). Characteristics of melt water discharge in the Glacier No. 1 basin, headwater of Urumqi River. *Journal of Hydrology*, 489, 180–188.
- Grove, J. M. (2004). *Little ice ages, ancient and modern*. London: Routledge.
- Guo, W. Q., Liu, S. H., Yao, X. J., Xu, J. L., Shangguan, D. H., Wu, L. Z., ... Wang, Y. (2014). *The Second Glacier Inventory Dataset of China (Version 1.0)*. Lanzhou: Cold and Arid Regions Science Data Center.
- Khromova, T. E., Dyurgerov, M. B., & Barry, R. G. (2003). Late-twentieth century changes in glacier extent in the Ak-shirak Range, Central Asia, determined from historical data and ASTER imagery. *Geophysical Research Letters*, 30(16), 5, Article Number: 1863.
- Koppes, M., Gillespie, A. R., Burke, R. M., Thompson, S. C., & Stone, J. (2008). Late Quaternary glaciation in the Kyrgyz Tien Shan. *Quaternary Science Reviews*, 27, 846–866.
- Li, Y. K., Liu, G. N., Chen, Y. X., Li, Y. N., Harbor, J., Stroeven, A. P., ... Cui, Z. J. (2014). Timing and extent of Quaternary glaciations in the Tianger Range, eastern Tian Shan, China, investigated using ¹⁰Be surface exposure dating. *Quaternary Science Reviews*, 98, 7–23.
- Li, Y. K., Liu, G. N., Kong, P., Harbor, J., Chen, Y. X., & Caffee, M. (2011). Cosmogenic nuclide constraints on glacial chronology in the source area of the Urumqi River, Tian Shan, China. *Journal of Quaternary Science*, 26, 297–304.
- Li, Y. K., Napieralski, J., & Harbor, J. (2008). A revised automated proximity and conformity analysis method to compare predicted and observed spatial boundaries of geologic phenomena. *Computers & Geosciences*, 34, 1806–1814.

- Li, Y. N., & Li, Y. K. (2014). Topographic and geometric controls on glacier changes in the central Tien Shan, China, since the Little Ice Age. *Annals of Glaciology*, 55(66), 177–186.
- Lioubimtseva, E., & Henebry, G. M. (2009). Climate and environmental change in arid Central Asia: Impacts, vulnerability, and adaptations. *Journal of Arid Environments*, 73(11), 963–977.
- Liu, C. H., & Han, T. D. (1992). Relation between recent glacier variations and climate in the Tien Shan Mountains, Central Asia. *Annals of Glaciology*, 16, 11–16.
- Liu, S. Y., Sun, W. X., Shen, Y. P., & Li, G. (2003). Glacier changes since the Little Ice Age maximum in the western Qilian Shan, northwest China, and consequences of glacier runoff for water supply. *Journal of Glaciology*, 49, 117–124.
- Matthes, F. E. (1939). Report of committee on glaciers. *Transactions American Geophysical Union*, 20, 518–523.
- Matthews, J. A., & Briffa, K. R. (2005). The Little Ice Age: Re-evaluation of an evolving concept. *Geografiska Annaler, Series A: Physical Geography*, 87(1), 17–36.
- Narama, C., Kondo, R., Tsukamoto, S., Kajiura, T., Ormukov, C., & Abdrakhmatov, K. (2007). OSL dating of glacial deposits during the last glacial in the Terskey-Alatoo Range, Kyrgyz Republic. *Quaternary Geochronology*, 2, 249–254.
- Paul, F., Barry, R. G., Cogley, J. G., Frey, H., Haeberli, W., Ohmura, A., ... Zemp, M. (2009). Recommendations for the compilation of glacier inventory data from digital sources. *Annals of Glaciology*, 50(53), 119–126.
- Paul, F., Huggel, C., & Kääb, A. (2004). Combining satellite multi-spectral image data and a digital elevation model for mapping debris-covered glaciers. *Remote Sensing of Environment*, 89(4), 510–518.
- Shi, Y. F., & Ren, J. W. (1990). Glacier recession and lake shrinkage indicating a climatic warming and drying trend in Central Asia. *Annals of Glaciology*, 14, 261–265.
- Solomina, O. N., & Alverson, K. (2004). High latitude Eurasian paleoenvironments: Introduction and synthesis. *Palaeogeography, Palaeoclimatology, Palaeoecology*, 209(1–4), 1–18.
- Solomina, O. N., Barry, R., & Bodnya, M. (2004). The retreat of Tien Shan glaciers (Kyrgyzstan) since the Little Ice Age estimated from aerial photographs, lichenometric and historical data. *Geografiska Annaler, Series A: Physical Geography*, 86(A2), 205–215.
- Sorg, A., Bolch, T., Stoffel, M., Solomina, O. N., & Beniston, M. (2012). Climate change impacts on glaciers and runoff in Tien Shan (Central Asia). *Nature Climate Change*, 2, 725–731.
- Stroeven, A. P., Hättestrand, C., Heyman, J., Kleman, J., & Morén, B. M. (2013). Glacial geomorphology of the Tian Shan. *Journal of Maps*, 9(4), 505–512.
- Sun, X. J., Shen, S. H., Leptoukh, G. G., Wang, P. X., Di, L. P., & Lu, M. Y. (2012). Development of a web-based visualization platform for climate research using Google Earth. *Computers & Geosciences*, 47, 160–168.
- Xu, X. K., & Yi, C. L. (2014). Little Ice Age on the Tibetan Plateau and its bordering mountains: Evidence from moraine chronologies. *Global and Planetary Change*, 116, 41–53.
- Yi, C. L., Liu, K. X., Cui, Z. J., Jiao, K. Q., Yao, T. D., & He, Y. Q. (2004). AMS radiocarbon dating of late Quaternary glacial landforms, source area of the Urumqi River, Tien Shan – a pilot study of ¹⁴C dating on inorganic carbon. *Quaternary International*, 121, 99–107.
- Yu, L., & Gong, P. (2012). Google Earth as a virtual globe tool for Earth science applications at the global scale: progress and perspectives. *International Journal of Remote Sensing*, 33(12), 3966–3986.
- Zech, R. (2012). A late Pleistocene glacial chronology from the Kitschi-Kurumdu Valley, Tien Shan (Kyrgyzstan), based on ¹⁰Be surface exposure dating. *Quaternary Research*, 77, 281–288.
- Zhao, J. D., Zhou, S. Z., He, Y. Q., Ye, Y. G., & Liu, S. Y. (2006). ESR dating of glacial tills and glaciations in the Urumqi River headwaters, Tianshan Mountains, China. *Quaternary International*, 144, 61–67.